THE JOURNAL OF PHYSICAL CHEMISTRY C

ARTICLE

pubs.acs.org/JPCC

Surface-Confined Pyrroloquinoline Quinone: Characterizations and Interactions with Copper Ions

Chong Mou Wang,* Shung-Yue Chung, Hsi-Jung Jao, and Wei-Hsiu Hung*

Department of Chemistry, National Taiwan Normal University, Taipei 116, Taiwan

Supporting Information

ABSTRACT: Inspired by the unique reactivity of the surface-bound quinone and copper cofactors in copper-containing amine oxidases, we investigated the interactions of pyrroloquinoline quinone (PQQ) with copper ions in solution and adsorbed on indium-doped tin oxide (ITO) electrodes. Characterizations based on atomic force microscopy, electrochemical mode scanning tunneling microscopy, and emission spectroscopy showed that when PQQ was reduced, the resulting two-electron transfer product, $PQQH_2$, could couple to 3-aminophenylboronic acid and therefore be tethered to ITO. $PQQH_2$ was also noticed to form multilayer adsorption on the electrodes, featuring reversible changes in adsorption and desorption with potential switching. X-ray photoelectron spectroscopic analysis and X-ray absorption near-edge-structure spectral measurements showed that both PQQ and $PQQH_2$ could interact with copper ions through the N-1 and N-6 sites. Because of this reactivity, the copper ion exhibited quenching effects on the photoexcited PQQ and $PQQH_2$ in solution and on ITO. In addition, current enhancement for $PQQ^{0/2-}$ was also noticed during the reduction of PQQ as copper ions were added, indicating that $PQQH_2$ could transfer electrons to Cu^{2+} ions. The electron transfer rate constant was estimated to be $\sim 10^{12}$ cm^6 mol^{-2} s^{-1} at pH 3. This electron transfer reaction, however, was less influential than the complexation counterpart in quenching the excited $PQQH_2$. We thus deduce that the electron transfer process may be less energetic or slower than the complexation counterpart or that it takes place only after the latter is complete.

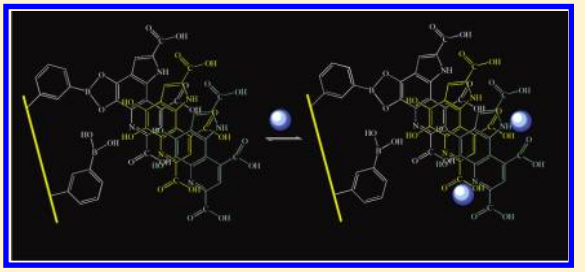

INTRODUCTION

Copper-containing amine oxidases (CAOs)[1−3] are novel quinoproteins, that are essential for aerobic organisms in growth, secondary metabolism, and physiological function regulation.[4,5] The functions of CAOs, although diversified with the source of the enzyme, are united in the deamination of primary amines with oxygen.[6] The catalytic cycle consists of the formation of aminoquinol and aldehyde and the oxidation of the aminoquinol back to the quinone with the release of hydrogen peroxide and ammonia.[1,2] The incorporated Cu(II) may stabilize the quinone cofactors and form intermediates with the semiquinone form of the quinone cofactors. This unique reactivity prompted us to investigate pyrroloquinoline quinone (PQQ), the only dissociable quinone cofactor, for its reactivity with copper ions in solution and adsorbed on electrodes.

PQQ is a redox coenzyme of various bacterial dehydrogenases,[7] efficient in bidirectional electron-transfer mediation.[8,9] In addition to its catalytic role, PQQ is also considered to be an essential nutrient for mammals.[10] It can form charge-transfer complexes with aromatic amino acids[11] and exists with affinities to metal ions such as Na^+ and Ca^{2+} and organic cations.[7] According to our study, PQQ can interact with copper ions in solution or adsorbed on electrodes, and the N-1 and N-6 sites are probably the reaction sites. Characterizations showed that when PQQ was reduced to quinol ($PQQH_2$), it formed a 1:1 adduct with 3-aminophenylboronic acid (APBA) via a coupling reaction between the dihydroxyl group and the boronic acid group in APBA. $PQQH_2$ could thus be tethered to the surface of electrodes such as indium-doped tin oxide (ITO). $PQQH_2$ showed affinities for copper ions and could donate electrons to Cu^{2+} ions as well, leading to current enhancement for $PQQ^{0/2-}$. This electron-transfer reaction could cause emission quenching for the excited $PQQH_2$. However, its impact was less effective than that of the complexation counterpart. Accordingly, the electron transfer between $PQQH_2$ and copper ion seems to be a slow process in comparison with the complexation counterpart, or it takes place only after the complexation reaction is complete as $PQQH_2$ encounters copper ions.

EXPERIMENTAL SECTION

Materials. 3-Aminophenylboronic acid hydrochloride (APBA, HCl salt), copper sulfate, sodium nitrite, and sodium borohydride were purchased from Aldrich. Methoxatin (PQQ) was supplied by Sigma and used as received without further purification. ITO glass squares (indium-doped, 0.7 mm thick, 20 Ω cm^{-2}) were obtained from Delta Technologies. $PQQH_2$ was synthesized by reacting

Received: August 28, 2010
Revised: November 13, 2010
Published: December 21, 2010

PQQ (1 mmol) with equimolar $NaBH_4$ in ethanol (95%, 50 mL) under nitrogen at 10 °C for 3 h. After quenching the unreacted $NaBH_4$ with NH_4Cl (0.1 M in water), the product was isolated and recrystallized in ethyl acetate and then stored under nitrogen. The NMR yield was ~85%.

Surface Modifications. Unless otherwise specified, APBA was modified on conductive ITO glass squares (0.5×0.5 cm^2) through a diazotization−cathodic reduction process.[12,13] Typically, APBA (1 mM) was mixed with equimolar $NaNO_2$ in 0.01 M HCl and then subjected to an immediate potential cycling from 0 to −0.6 V versus SCE for 10 cycles with ITO electrodes at a constant scan rate (20 mV/s). The resultant electrodes (ITO|APBA) were then brought to solutions containing 0.1 M KCl and 1×10^{-4} M PQQ for PQQ modification. This process was carried out through electrolysis (potential step, 30 s) or potential cycling between 0.5 and −0.5 V at a scan rate of 50 mV/s. Because the reduction of PQQ to $PQQH_2$ is a two-electron, two-proton process and PQQ exhibits the highest electrochemical activity around pH 3,[14] the pH in this case was controlled at a value of 3 and for the latter characterization. This acidic environment also effectively prevented copper ion from precipitation. The PQQ-modified electrodes (ITO|APBA|$PQQH_2$) were then subjected to characterizations with cyclic voltammetry (CV) or linear sweep voltammetry (LSV) in 0.1 M KCl (pH 3) or atomic force microscopy (AFM) in air.

Apparatus. A PAR 283 potentiostat (EG & G) was used for electrode modifications and electrochemical characterizations. Unless otherwise specified, all electrochemical experiments were carried out in a nitrogen environment in a one-compartment cell with a Pt counter electrode and an SCE reference electrode. Emission analysis was performed on an Aminco-Bowman luminescence spectrophotometer (series 2) in conjunction with a Hamamatsu R2949 photomultiplier tube. Diffuse reflectance emission spectra were also measured with this photometer in conjunction with a Y-type optical fiber (Oriel M 77404). UV−vis absorption spectra were recorded with a UV−vis absorption spectrometer (JASCO 7850) and a standard rectangular ($1 \times 1 \times 5$ cm^3) quartz cuvette as the sample holder. AFM and electrochemical scanning tunneling microscopy (EC−STM) were performed on a Nanoscope III E AFM (Digital Instruments, Santa Barbara). For roughness analysis, we scratched the surface in contact mode. The height profile across the scratch on the film gave the film thickness, which roughly equaled the surface roughness given by the tapping mode AFM. For EC−STM, a home-built preamplifier and Pt/Ir tips were employed for current measurements. In this case, a silver wire served as the pseudo-reference. The potential was calibrated against ferrocene. X-ray photoelectron spectroscopic (XPS) and X-ray absorption near-edge-structure spectral (XANES) measurements were conducted at the National Synchrotron Radiation Research Center (NSRRC), Taiwan, with collection in a total-electron-yield mode using a high-energy spherical-grating monochromator (HSGM, 6 m) beamline. For the N K-edge analysis, PQQ (1 mmol) and varying amounts of $CuSO_4$ (0−10 mmol) were dissolved in 10 mL of HCl (1 mM) to give desired mole ratios. $CuSO_4$ (1 mmol) was also dissolved with varying amounts of PQQ (0−10 mmol) in 10 mL of HCl for the Cu 3p binding energy measurements. The resultant solutions were then pipetted (10 $\mu L/cm^2$) and dipped on ITO glass squares and dried under N_2. For XPS, the incident angle of the photons was 55° from the surface normal. Emitted photoelectrons were collected with the electron analyzer normal to the sample surface in an angle-integrated mode.

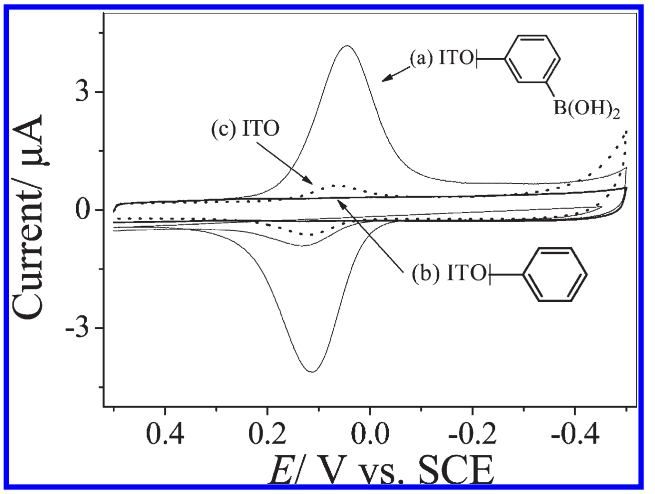

Figure 1. Surface waves imprinted on (a) ITO|APBA, (b) ITO|aniline, and (c)ITO after the electrodes being subjected to potential cycling in 0.1 M KCl + 1×10^{-4} M PQQ (pH 3) from 0.5 to −0.5 V versus SCE for 10 cycles.

RESULTS AND DISCUSSION

In surface-modifying PQQ, APBA is a useful molecular adhesive. Figure 1 shows that when APBA was premodified on ITO electrodes through a diazotization−cathodic reduction process, the resultant electrodes (denoted ITO|APBA) were imprinted with a pair of surface waves characteristic of PQQ/$PQQH_2$ (trace a)[14,15] after the electrodes were subjected to potential cycling in 1×10^{-4} M PQQ (pH 3) within ±0.5 V versus SCE. (See Figures S1 and S2 of the Supporting Information for the dependence on pH and scan rate.)

$$PQQ + 2e^- + 2H^+ \rightleftharpoons PQQH_2 \qquad (1)$$

Aniline did not show any waves in this aspect when substituted for APBA (trace b). Although bare ITO displayed similar waves on its surface (trace c), the waves in terms of amplitude were relatively insignificant in comparison with those on ITO|APBA. The surface waves imprinted on ITO|APBA are thus considered to result from a coupling reaction between the quinol form of PQQ (denoted $PQQH_2$) and the boronic acid group in APBA (Scheme 1).[16] Surface roughness analysis of ITO and ITO|APBA supported this hypothesis (Figure S3 of the Supporting Information). ITO electrodes changed roughness from 1.4 to 3.0 nm after being modified with APBA (Figure 2). The resultant ITO|APBA electrodes further changed roughness to ~7 nm after being kept in 1×10^{-4} M PQQ and biased at potentials (potential step) more negative than the formal potential of PQQ ($E^{o\prime}$ = ~0 V versus SCE); the AFM images inset in Figure 2 contrast the topographic difference between the cases of 0.3 and −0.3 V. The surface density (Γ) of $PQQH_2$ on each ITO|APBA electrode was also calculated on the basis of the faradic currents subtracted from the reductive wave, revealing similar dependence on the applied bias (E). The results in terms of Γ versus E are plotted in Figure 3 with the mole ratio (α) for $PQQH_2$

$$\alpha = c_{PQQH_2}/(c_{PQQ} + c_{PQQH_2}) = \{1+\exp[2F(E-E^{o\prime})/RT]\}^{-1} \qquad (2)$$

Here c_{PQQ} and c_{PQQH_2} stand for the concentrations of PQQ and $PQQH_2$ designated by each potential. Both Γ and α trend to

Scheme 1. Schematic Illustrations for the Coupling Reaction between $PQQH_2$ and APBA on ITO and the Accompanying Multilayer Adsorption

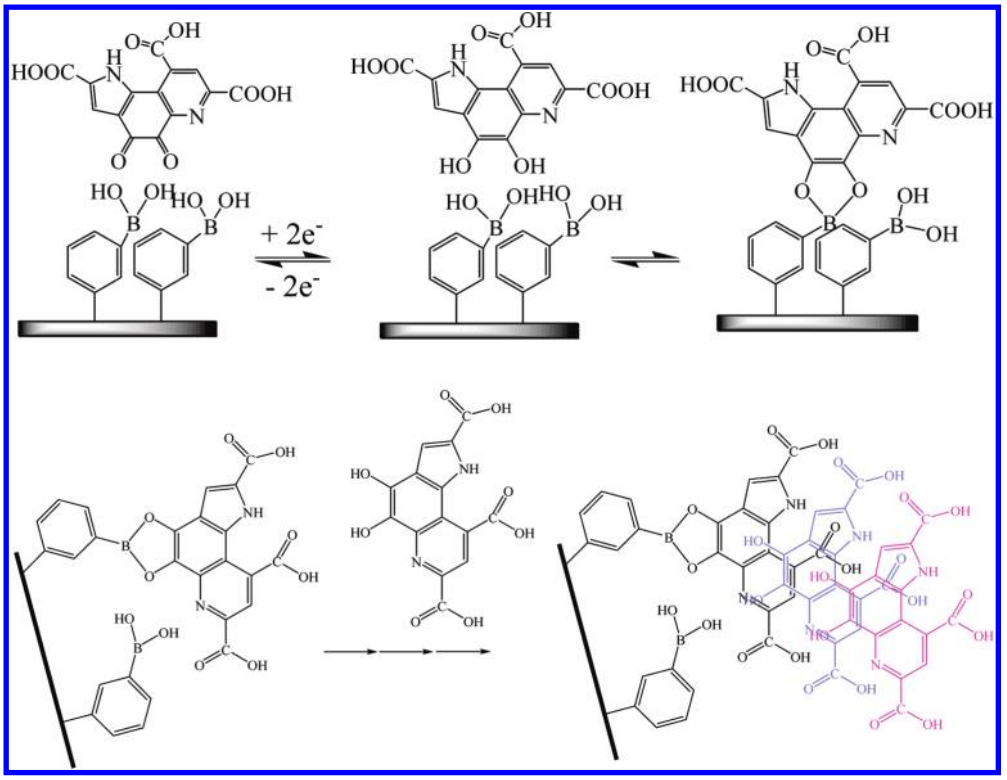

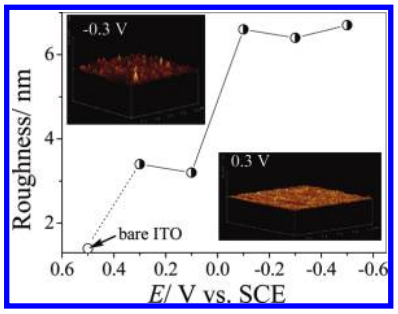

Figure 2. Roughness of ITO|APBA recorded after being biased at varying potentials (potential step; 30 s) in 1×10^{-4} M PQQ. Insets show the topographic contrast between the cases of −0.3 and 0.3 V.

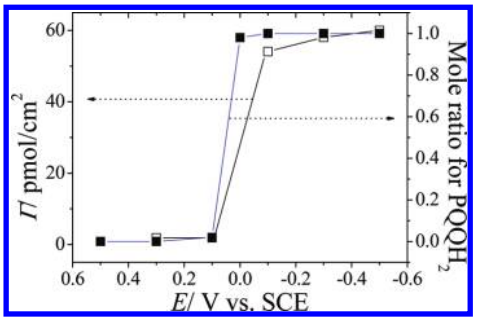

Figure 3. Correlations between Γ and α and *E*. Conditions as in Figure 2.

saturation (~60 pmol/cm^2) as $E \rightarrow -\infty$. $PQQH_2$ is thus shown to play a key role in the proposed coupling reaction. Verification of Scheme 1 showed that without PQQ, ITO|APBA did not change in roughness (Figure S4 of the Supporting Information). Chemically synthesized $PQQH_2$ could interact with ITO|APBA under open-circuit conditions. In this case, the resultant electrodes (denoted ITO|APBA|$PQQH_2$) gained ~3 nm in roughness and showed a pair of surface waves (Figure S5 of the Supporting Information) similar to those shown in Figure 1a. Many other anthraquinones such as 1,10-phenanthroline-5,6-dione and 9,10-phenanthrenequinone also exhibited similar affinities to ITO|APBA after being cathodically reduced (Figure S6 of the Supporting Information). The mechanism proposed in Scheme 1 is thus considered to be possible.

The roughness difference between ITO|APBA and ITO|APBA|$PQQH_2$ shown in Figure 2, however, is less compatible with the molecular size of $PQQH_2$ (~0.5 nm). We considered this inconsistency to result from a multilayer adsorption of $PQQH_2$ onto the electrode through intermolecular interactions between $PQQH_2$, such as $\pi-\pi$ stacking and the extensive hydrogen-bond networks[9] proposed in Scheme 1, using the surface-bound $PQQH_2$ as the adsorption sites. This postulate is in accordance with the surface density of $PQQH_2$ on ITO|APBA (~10 monolayers estimated under the assumption that each $PQQH_2$ are separated by 3 nm) and also accounts for the poor adsorption of $PQQH_2$ on ITO (Figure 1c) and the indifferent affinity of $PQQH_2$ for ITO when aniline was substituted for APBA (Figure S7 of the Supporting Information). The physically adsorbed $PQQH_2$ seemed to be reversible in desorption and adsorption. The EC−STM analysis of ITO|APBA in 1×10^{-4} M PQQ (Figure 4) showed that the roughness of the electrode, *r*, altered correspondingly with the switching in the bias applied to the electrode, despite the *r*−*E* loops not being perfectly

dx.doi.org/10.1021/jp1081774 |*J. Phys. Chem. C* 2011, 115, 1978–1984

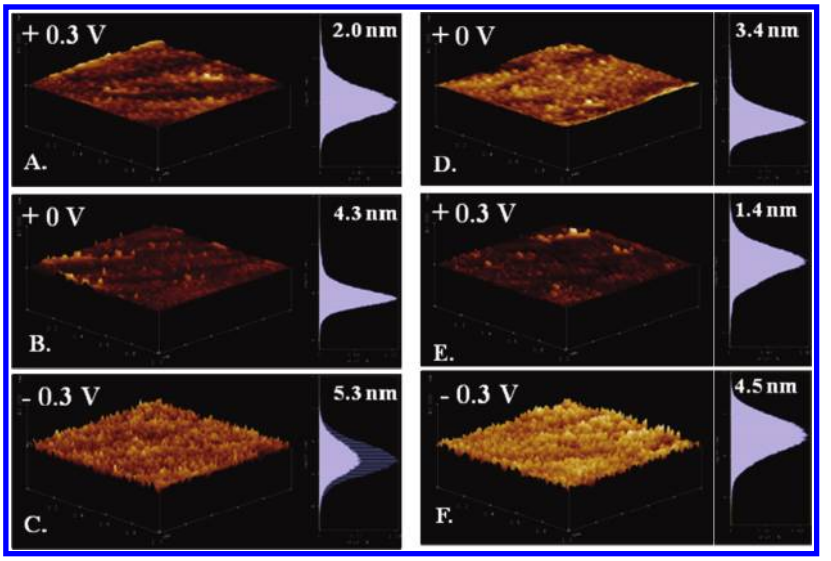

Figure 4. EC−STM images of ITO|APBA recorded in situ in 0.1 M KCl + 0.1 mM M PQQ (pH 3) at varying potentials. Image scan rate: 1 Hz; size: 1 μm^2; tip current: 0.2 nA; tip bias: 0.2 V.

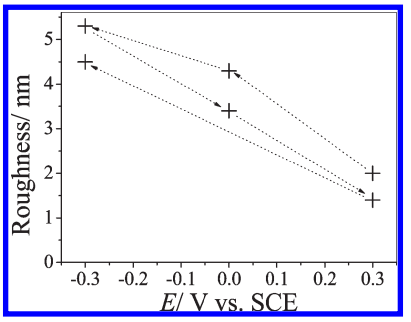

Figure 5. Changes in the roughness of ITO|APBA with *E*. Conditions as in Figure 4.

superimposed (Figure 5). The variations in *r* are less likely to arise from the fragility of the APBA film and more likely to be due to the desorption of PQQ and the adsorption of $PQQH_2$ governed by reaction 1 because the surface waves of $PQQ^{0/2-}$ remained almost intact after the EC−STM experiments.

XPS failed to provide evidence of a coupling reaction between $PQOH_2$ and APBA because of a poor distinction between the boron atoms (E_b: 188 eV) in APBA and the $PQQH_2$ adduct. This problem, in fact, also exists between APBA and other esters such as 3-aminophenylboronic acid pinacol ester (Figure S8 of the Supporting Information). Nevertheless, $PQQH_2$ showed drastic changes in the emission spectra (λ_{em}: 475 nm; λ_{ex}: 365 nm) as APBA was incorporated (Figure 6A). The intensity increased with [APBA] and tended to saturation for [APBA] > 0.2 mM. In this case, the UV−vis absorption spectra of $PQQH_2$ also changed correspondingly. In contrast with $PQQH_2$, PQQ showed no alterations in these aspects (Figure 6B). APBA does not emit under excitation at 365 nm. The emission enhancement shown in Figure 6A is thus considered to arise from a reduction in the vibrational relaxation associated with the excited $PQQH_2$ because of the formation of bulky, rigid products with APBA

$$PQQH_2 + n\text{APBA} \rightarrow \text{product} \qquad (3)$$

$$K = [\text{product}]/\{[PQQH_2][\text{APBA}]^n\} \qquad (4)$$

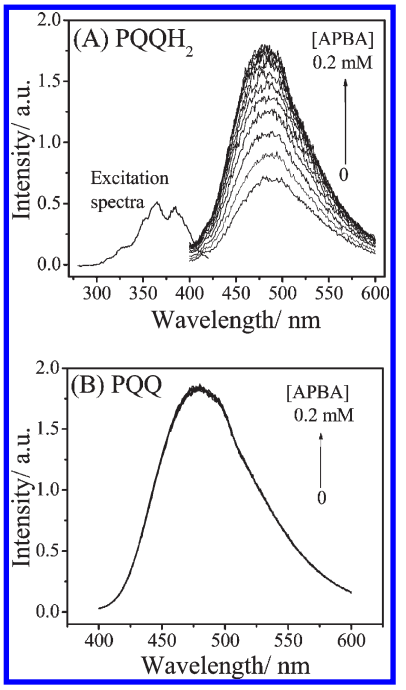

Figure 6. Emission spectra of (A) $PQQH_2$ and (B) PQQ (1×10^{-4} M each) with varying amounts of APBA.

Provided that the intensity of the 475 nm band (denoted *F*) is contributed by $PQQH_2$ and the reaction product

$$F = k_1[PQQH_2] + k_2[\text{product}] \qquad (5)$$

F is expected to comply with the following relationship

$$F_o/\Delta F = [k_1/(k_2 - k_1)]\{K^{-1}[\text{APBA}]^{-n} + 1\} \qquad (6)$$

Here F_o is the initial intensity, ΔF is defined as $(F - F_o)$, k_1 and k_2 are the proportionality constants for $PQQH_2$ and the product, respectively, and *n* is the stoichiometric ratio between $PQQH_2$ and APBA. According to the best linear fit for the plots of $F_o/\Delta F$ versus

dx.doi.org/10.1021/jp1081774 |J. Phys. Chem. C 2011, 115, 1978–1984

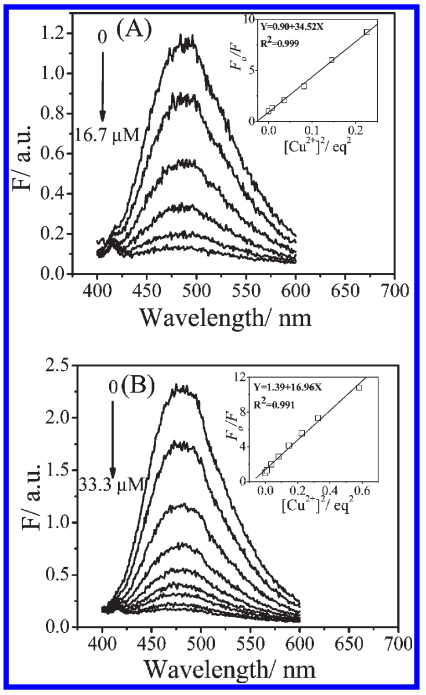

Figure 7. Emission spectra of (A) 1×10^{-4} M $PQQH_2$ and (B) 1×10^{-4} M $PQQH_2 + 2 \times 10^{-4}$ M APBA with varying amounts of copper ions. Insets show the correlations between F_o/F and $[Cu^{2+}]^2$. 1 equiv = 35 μM.

$[APBA]^{-n}$ (Figure S9 of the Supporting Information), each APBA couples to one $PQQH_2$ ($n = 1$; $K = 6 \times 10^5$ M^{-1}).

When PQQ was brought into contact with copper ions, its emission spectra decreased in intensity with an increase in $[Cu^{2+}]$ (Figure S10A of the Supporting Information), leading to the following Stern−Volmer-type relationship

$$F_o/F = 1 + K_Q[Cu^{2+}]^2 \quad (7)$$

Here F_o and F stand for the peak intensities of the emission band of PQQ in the absence and the presence of copper ions, respectively, and K_Q is the quenching constant. For this quenching behavior, we examined the UV−vis absorption spectra of PQQ (Figure S10B of the Supporting Information) and compared the energy levels of $PQQ/PQQH_2$ and $PQQ^*/PQQH_2$ with that of $Cu^{2+/+}$ (Figure S11 of the Supporting Information). The UV−vis absorption spectra of PQQ changed correspondingly during the addition of Cu^{2+} ions, and the energy level for $PQQ/PQQH_2$ is relatively more negative than $Cu^{2+/+}$ in terms of potential. In view of these facts, dynamic quenching, such as charge transfer, and steady-state quenching, such as the complexation reaction described in eq 8, may be the cause of the emission quenching. For the latter case, K_Q is equivalent to the formation constant, K_f.

$$PQQ + yCu^{2+} \rightleftharpoons \text{complex}, K_f \quad (8)$$

Like PQQ, the solution $PQQH_2$ could also interact with copper ion (Figure 7A), even in the presence of APBA (Figure 7B). The values of y and K_Q, according to eqs 7 and 8, were estimated to be (2 and 3) $\times 10^{10}$ M^{-2} for the case without APBA and 2 and 1×10^{10} M^{-2} as with APBA. Both are quite close to the values found with PQQ ($y = 2$, $K_Q = 2 \times 10^9$ M^{-2}).

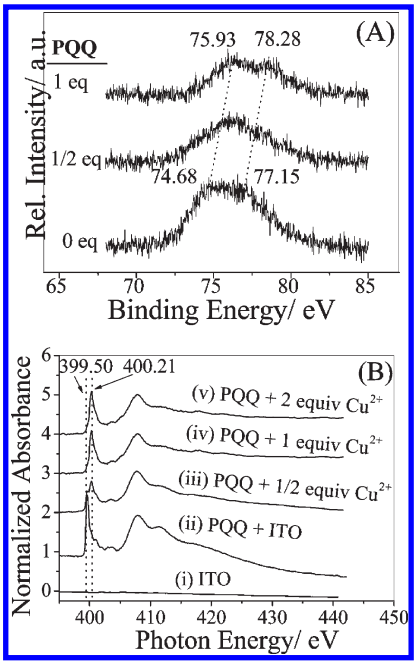

Figure 8. XPS spectra for copper sulfate with varying amount of (A) PQQ and (B) N K-edge XANES for PQQ with varying amount of Cu^{2+} ions; 1 equiv =1 μmol/cm^2.

According to these data, PQQ and $PQQH_2$ are likely to interact with Cu^{2+} in a similar way, as follows

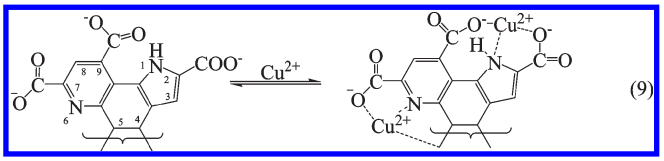

(9)

For reaction 9, XPS analysis (Figure 8) of copper showed that the 3p electron binding energies ($3p_{3/2}$ and $3p_{1/2}$) shifted from 74.68 and 77.15 eV to 75.93 and 78.28 eV, respectively, as Cu^{2+} was incorporated with 1 equiv of PQQ. XANES for PQQ also indicated that the N K-edge shifted from 399.5 to 400.21 eV as PQQ was incorporated with 2 equiv of Cu^{2+}. Although we are short of evidence of which nitrogen, N-6 or N-1, is responsible for the energy shift, both are likely the reaction sites after taking into consideration the value of y determined by the emission data recorded in Figure 7 and the interaction reported between PQQ and Ca^{2+}.[17] We also attempted to elucidate the role of oxygen through XANES. The conclusion is not certain because of a difficulty in specifying oxygen atoms and the interference from the background. Despite this, because $PQQH_2$ resulted in similar K_Q and y regardless of the presence of APBA, the C═O groups on C-4 and C-5 are not likely to participate in reaction 9. For this reason, $PQQH_2$, as adsorbed ITO|APBA, showed similar sensitivity to copper ions. The associated diffuse-reflectance emission spectra decreased systematically in intensity with $[Cu^{2+}]^2$, as shown in Figure 9, similar to that observed with the solution counterpart despite the half-height width being wider.

Apart from reaction 9, $PQQH_2$ also exhibited electrochemical reactivity toward copper ions. Figure 10 shows that when ITO|APBA|$PQQH_2$ was subjected to potential cycling in 0.1 M KCl (pH 3) with the presence of copper ion, the resulting cathodic current increased systematically with the concentration of the Cu^{2+} ions (inset). This behavior was blurred as carbon electrodes

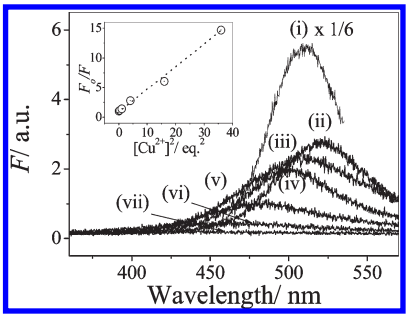

Figure 9. Diffuse-reflectance emission spectra for ITO|APBA in the presence of 0.1 mM $PQQH_2$ (trace (i)). Traces (ii−vii) show the spectra revealed from the resultant electrode in a pH 3 solution free of $PQQH_2$ with varying amounts of copper ions: (ii) 0, (iii) 0.5, (iv) 1.0, (v) 2.0, (vi) 4.0, and (vii) 6.0 equiv (1 equiv $=1 \times 10^{-4}$ M). Inset shows the relationship between F_o/F and $[Cu^{2+}]^2$.

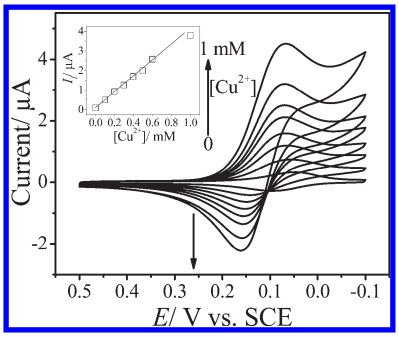

Figure 10. CV curves recorded with an ITO|APBA|$PQQH_2$ electrode in 0.1 M KCl (pH 3) with varying amounts of Cu^{2+} ions (0 to 1 mM) at a scan rate of 5 mV/s. Inset shows the linear relationship between the currents sampled at −0.05 V and $[Cu^{2+}]$.

were substituted for ITO because the reduction of copper ions occurred at a potential more positive than that for $PQQ^{0/2-}$. In view of this, the current enhancement is considered to be unlikely to result from current overlapping or the formation of semiquinone because copper ions contributed only insignificant currents to ITO or ITO|APBA near the formal potential of $PQQ^{0/2-}$ (~0.05 V vs SCE) as PQQ was excluded (Figure S12 of the Supporting Information) and $PQQ^{0/2-}$ did not split into two waves during the incorporation of copper ions. Quinone often features two distinct one-electron transfer waves in aprotic systems.[18] However, the strong affinity of the quinol hydroxyls for protons leads the second electron transfer step in protic media to be more energetically favorable than the first one at pH values below the pK_a values of the quinol hydroxyls. A two-electron transfer process thus results unless the system is less acidic or incorporates supporting electrolytes that can interact with or stabilize the semiquinone.[19,20] The current enhancement is thus considered to derive from reactions 1 and 10

$$PQQH_2 + 2Cu^{2+} \rightarrow PQQ + 2Cu^{+} + 2H^{+}, k \qquad (10)$$

Here k stands for the forward reaction rate constant. On the basis of the proposed mechanism and the thin-layer-cell approach,[21,22] under the assumption that the cell width, that is, the thickness of the $PQQH_2$ layer on ITO|APBA|$PQQH_2$, is smaller than the diffusion distance for PQQ and $PQQH_2$, the concentration profiles of PQQ and $PQQH_2$ become functions of time only, independent of distance, and the current (I) can then be solved from the following equation[21]

$$I/nFV = -\partial[PQQ]/\partial t + k[PQQH_2][Cu^{2+}]^2 \qquad (11)$$

Assuming that $[PQQ]$ and $[PQQH_2]$ on ITO|APBA|$PQQH_2$ are conserved and comply with the Nernst equation, then

$$[PQQ] + [PQQH_2] = c \qquad (12)$$

$$[PQQ]/[PQQH_2] = \theta = \exp[nF/RT(E_i - vt - E^{o\prime})] \qquad (13)$$

I is resolved to be

$$I = n^2F^2Vvc[\theta/(\theta+1)^2]/RT + nFVck[Cu^{2+}]^2/(\theta+1) \qquad (14)$$

or more properly

$$I = n^2F^2Av\Gamma[\theta/(\theta+1)^2]/RT + nFA\Gamma k[Cu^{2+}]^2/(\theta+1) \qquad (15)$$

Here E_i stands for the initial potential, V is the volume of the $PQQH_2$ layer on ITO|APBA|$PQQH_2$, v is the scan rate, c is the total concentration of PQQ and $PQQH_2$ in the cell, A is the area of the electrode, and Γ is the surface density of the adsorbed PQQ and $PQQH_2$. As E approaches $-\infty$ ($\theta \rightarrow 0$), I reaches a limiting value, I_l

$$I_l = nFA\Gamma k[Cu^{2+}]^2 \qquad (16)$$

By approximating the currents at −0.05 V to I_l, we plotted I_l against $[Cu^{2+}]^m$ (m = 1, 2, and 3). The best linear fit was found to exist at m = 1 (inset, Figure 10). This result contrasts greatly with the results predicted by eq 16, suggesting that most PQQ and $PQQH_2$ molecules on ITO|APBA|$PQQH_2$ might not be rigidly held, that is, possess some degrees of freedom in motion. Accordingly, we solved Fick's second law for PQQ and $PQQH_2$ provided that they are semidiffusional.

$$\partial[PQQ]/\partial t = D_{PQQ}(\partial^2[PQQ]/\partial x^2) + k[PQQH_2][Cu^{2+}]^2 \qquad (17)$$

$$\partial[PQQH_2]/\partial t = D_{PQQH_2}[\partial^2[PQQH_2]/\partial x^2] - k[PQQH_2][Cu^{2+}]^2 \qquad (18)$$

The following current−voltage relationship is expected at a very slow scan rate ($v \rightarrow 0$)

$$I = nFAc_{PQQ}(D_{PQQ}k[Cu^{2+}]^2)^{1/2}/(1+\theta') \qquad (19)$$

$$\theta' = \exp[(nF/RT)[E - E^{o\prime} + (RT/nF)\ln(D_{PQQ}/D_{PQQH2})^{1/2}] \qquad (20)$$

Here D_{PQQ} and D_{PQQH_2} stand for the diffusion coefficients of PQQ and $PQQH_2$. As $E \rightarrow -\infty$, $\theta' \rightarrow 0$, the current reaches the limiting value, I_l

$$I_l = nFAc_{PQQ}(D_{PQQ}k[Cu^{2+}]^2)^{1/2} \qquad (21)$$

As predicted, control experiments with bare ITO in 1×10^{-4} M PQQ (pH 3) showed a linear correlation between I_l and $[Cu^{2+}]$ (Figure S13 of the Supporting Information), similar to that displayed in Figure 10. The forward reaction rate constant, k, was estimated to be ~10^{12} cm^6 mol^{-2} s^{-1} under the assumption that $D_{PQQ} \approx 10^{-6}$ cm^2 s^{-1}. Although the $PQQH_2$ moieties on ITO|

dx.doi.org/10.1021/jp1081774 |J. Phys. Chem. C 2011, 115, 1978–1984

APBA|$PQQH_2$ are not ideally stationary and the proposed electrocatalytic (EC′) mechanism has not been fully characterized, these results strongly suggest that Cu^{2+} ion can serve as an electron acceptor for $PQQH_2$. In this case, the emission quenching recorded in Figure 7 might also result from reaction 10. Provided that reactions 9 and 10 all participate in the emission quenching, the quenching law can be rewritten as follows

$$F_o/F = \{1 + K_Q[Cu^{2+}]^2\}\{1 + K_{ET}[Cu^{2+}]^2\} \quad (22)$$

$$(F_o/F - 1)/[Cu^{2+}]^2 = K_Q + K_{ET} + K_Q K_{ET}[Cu^{2+}]^2 \quad (23)$$

Here K_{ET} stands for the apparent equilibrium constant, that is, the impact factor of reaction 10 on $PQQH_2$*. According to the slope and intercept of the plots of $(F_o/F - 1)/[Cu^{2+}]^2$ against $[Cu^{2+}]^2$, $K_Q + K_{ET} \approx 3 \times 10^{10}\ M^{-2}$, approximately equaling K_Q ($3 \times 10^{10}\ M^{-2}$). Accordingly, $K_{ET} \ll K_Q$. Reaction 10 is thus shown to be far less significant than reaction 9. The electron transfer between $PQQH_2$ and copper ion is thus considered to be a process less energetic or slower than the complexation reaction or not to occur until the complexation process is complete.

CONCLUSIONS

PQQ, as reduced to $PQQH_2$, can be coupled to APBA and therefore surface-bound on ITO electrodes. Like PQQ, $PQQH_2$, either in solution or surface-bound on ITO, may complex with copper ions. The N-6 and N-6 sites are probably the reaction sites. This complexation reaction leads to emission quenching for PQQ and $PQQH_2$ because they are photochemically excited. The quenching constants are $\sim 10^{10}\ M^{-2}$ for both cases. Because the potential for $PQQ^{0/2-}$ is more negative than $Cu^{2+/+}$, PQQ, in solution or adsorbed on ITO, can also donate electrons to Cu^{2+} ions as being cathodically reduced, leading to current enhancement for $PQQ^{0/2-}$. The forward electron-transfer rate constant is $\sim 10^{12}\ cm^6\ mol^{-2}\ s^{-1}$. In theory, this electron transfer reaction can also cause emission quenching for the excited $PQQH_2$. It was found to be less influential than the complexation reaction. For this, we consider that the electron transfer between $PQQH_2$ and copper ion is a slow process in comparison with the complexation reaction or that it takes place only when the complexation process is complete.

ASSOCIATED CONTENT

Supporting Information. Surface waves on ITO|APBA|$PQQH_2$ and the pH and scan-rate dependence, AFM images of ITO|APBA, surface waves imprinted on ITO|APBA, roughness of ITO|APBA, contrasts between the topographic images and roughness of ITO|APBA, XPS for APBA and 3-aminophenylboronic acid pinacol ester, plots of $F_o/\Delta F$ versus $[APBA]^{-n}$, emission and UV−vis spectra for PQQ, energy levels for PQQ/$PQQH_2$, PQQ*/$PQQH_2$, and Cu^{2+}/Cu^{+}, representative LSV and CV curves, and plots of $(F_o/F-1)/[Cu^{2+}]^2$ against $[Cu^{2+}]^2$. This material is available free of charge via the Internet at http://pubs.acs.org.

ACKNOWLEDGMENT

We acknowledge financial support from the National Science Council, Republic of China (grant number: 96-2113-M-003-008-MY3; 99-2113-M-003-008-MY3).

REFERENCES

(1) Anthrony, C. *Biochem. J.* **1996,** *320,* 697.
(2) Mure, M. *Acc. Chem. Res.* **2004,** *37,* 131.
(3) Leitner, D. M.; Straub, J. E. *Proteins: Energy, Heat and Signal Flow*; CRC Press: Boca Raton, FL, 2009.
(4) Mure, M.; Mills, S. A.; Klinman, J. P. *Biochemistry* **2002,** *41,* 9269.
(5) Camakaris, J.; Voskoboinik, I.; Mercer, J. F. *Biochem. Biophys. Res. Commun.* **1999,** *261,* 225.
(6) Mondovi, B. *Structure and Function of Amine Oxidases*; CRC Press: Baton Rouge, LA, 1986.
(7) Gallop, P. M.; Pax, M. A.; Flückiger, R.; Stang, P. J.; Zhdankin, V. V.; Tykwinski, R. R. *J. Am. Chem. Soc.* **1993,** *115,* 11702.
(8) Yu, E. H.; Scott, K. *Energies* **2010,** *3,* 23.
(9) Katz, E.; Willner, I. *J. Am. Chem. Soc.* **2003,** *125,* 6803.
(10) Kasahara, T.; Kato, T. *Nature* **2003,** *422,* 832.
(11) Ishida, T.; Doi, M.; Tomita, K.; Hayashi, H.; Inoue, M.; Urakami, T. *J. Am. Chem. Soc.* **1989,** *111,* 6822.
(12) Wu, S.-W.; Huang, H.-Y.; Guo, Y. C.; Wang, C. M. *J. Phys. Chem. C* **2008,** *112,* 9370.
(13) March, G.; Reisberg, S.; Piro, B.; Pham, M.-C.; Fave, C.; Noel, V. *Anal. Chem.* **2010,** *82,* 3523.
(14) Jao, H.-J.; Tsai, P.-Y.; Wang, C. M. *J. Electroanal. Chem.* **2007,** *606,* 141.
(15) Duine, J. A.; Frank, J.; Verwiel, P. E. J. *Eur. J. Biochem.* **1981,** *118,* 395.
(16) Deore, B.; Freund, M. S. *Analyst* **2003,** *128,* 803.
(17) White, S.; Boyd, G.; Mathews, F. S.; Xia, Z.-X.; Dai, W.-W.; Zhang, Y.-F.; Davison, V. L. *Biochemistry* **1993,** *32,* 12955.
(18) Rich, P. R. *Biochim. Biophys. Acta* **2004,** *1658,* 165.
(19) Quan, M.; Sanchez, D.; Wasylkiw, M. F.; Smith, D. K. *J. Am. Chem. Soc.* **2007,** *129,* 12847.
(20) Gupta, N.; Linschitz, H. *J. Am. Chem. Soc.* **1997,** *119,* 6384.
(21) Shyu, S.-C.; Wang, C. M. *J. Electrochem. Soc.* **1997,** *144,* 3419.
(22) Bard, A. J.; Faulkner, L. R. Chapter 11. In *Electrochemical Methods: Fundamentals and Applications*, 2nd ed.; Wiley: New York, 2001; pp 452−458.